# Unidimensional models of the acoustic propagation in axisymmetric waveguides

Thomas Hélie

*IRCAM, centre G. Pompidou, CNRS UMR 9912, Équipe analyse-synthèse,*

*1 Place Igor Stravinsky, 75004 Paris, France**

Received:

Short title: 1D waveguide modelling

*Electronic address: `Thomas.Helie@ircam.fr`; University: Université de Paris XI

## Abstract

This paper presents a rigorous modelling of the linear acoustic propagation in axisymmetric waveguides, the pressure depending on a single space variable. The approach consists of writing the wave equation and the boundary conditions for a coordinate system rectifying the isobaric map at each time. The 2D-dependence of the problem is thus transferred from the pressure to the coefficients of the wave equation. From this result, an exclusively geometrical necessary condition is deduced for the admissibility of isobaric maps. However, the knowledge of the waveguide geometry is not sufficient to separate the pressure and the isobaric map solutions. In order to develop a unidimensional wave equation, a geometrical hypothesis is discussed. For lossless and motionless rigid waveguides, the deduced equation leads to exact results for tubes and cones. It may be interpreted as a Webster equation for a particular coordinate system so that the particular profiles for which analytical solutions of the pressure exist are redefined. The wave equation is also established for large pipes with visco-thermal losses and, more generally, for mobile walls having a small admittance. The compatibility of the geometrical hypothesis with the exact model is specified for this general case.


PACS numbers: 43.20.Mv, 43.20.Bi

## INTRODUCTION

This work deals with the derivation of models accounting for the acoustic propagation in axisymmetric waveguides and which depend on a single spatial variable. The first establishment of such 1D-models is due to Bernoulli[1] and Lagrange[2], even if the corresponding equation is commonly mentioned as the Webster equation[3]. This equation has been extensively investigated, witnessed by the bibliography compiled by Eisner[4], and the various geometrical hypotheses used for its derivation have been periodically discussed. Thus, planar wavefronts were contested by Lambert[5] and Weibel[6] who postulated spherical ones. They reported the inadequacy of the first assumption, exhibiting the fact that wavefronts may be orthogonal to any curved rigid wall. The quasi-sphericity was experimentally confirmed for a horn profile in the low frequency range by Benade and Janson[7]. Later, Putland[8] looked for necessary and sufficient conditions for a propagative acoustic mode to be spatially dependent on a single parameter. He pointed out that one-parameter acoustic fields obey a Webster equation and exhibited parallel planes, coaxial cylinders, and concentric spheres as the only possible corresponding potential surfaces. Nevertheless, even if finding a general 1D-modelling is hopeless and incites on other approaches[9,10], the simplicity of the Webster equation still stimulates the search for more accurate 1D-models. Thus, Agulló, Barjau, and Keefe[11] recently assumed the time-invariance of equipotential surfaces and developed 1D-modellings for both spherical surfaces and oblate ellipsoidal ones.

In this paper, a local geometrical hypothesis is proposed, namely, the quasi-sphericity of isobars near the wall. This hypothesis agrees with Benade and Janson's experiment[7] but does not require the wavefronts to be fixed. The general method relies on a time-domain wave equation established for a coordinate system locally rectifying the isobaric map at each time. The rectification ensures that the pressure is reduced to a 1D-function, but, concurrently, it transfers the 2D-dependence of the pressure to the coefficients of the isobaric wave equation. Establishing 1D-models requires making an assumption. The quasi-sphericity hypothesis is chosen as a natural extension of the property satisfied by plane and spherical waves travelling in cylinders and cones, respectively. Moreover, it does not resort to integral equations or averaging operators as usual, and makes the rectification method able to treat the case of rigid immobile walls as well as that of moving walls with a small admittance.

The structure of the paper is as follows: Sec. I presents the problem statement. Sec. II establishes all the exact derivations. General geometrical definitions are presented. The wave equation is expressed in a coordinate system which locally rectifies the isobaric map at each time. An admissibility condition necessarily satisfied by any isobaric map is then deduced. The case of globally time-invariant isobaric maps is investigated. Sec. III develops a 1D-model for rigid motionless walls. The geometrical hypothesis is first detailed. The derived 1D-model is proven to be equivalent to the Webster equation for which the longitudinal coordinate measures the arc length of the wall. The validity of both the hypothesis and the model is discussed. The particular profiles for which analytical solutions of the pressure exist are then redefined. Finally, Sec. IV extends the 1D-modelling to the cases of mobile walls having small admittances. The model is first derived, the compatibility of the geometrical hypothesis with this generalization is detailed, and the particular cases of mobile rigid walls and of visco-thermal boundary layers are investigated.

## I. PROBLEM STATEMENT

Throughout this paper, the problem considered is the linear acoustic propagation in guides that are symmetrical with respect to the longitudinal axis $(Oz)$. Only axisymmetric excitations are considered so that the whole problem is axisymmetric.

### A. Basic equations

For adiabatic lossless media, the equation of mass conservation[12]

$$\rho_0 c^2 \operatorname{div}(\mathbf{v}) = -\partial_t p, \tag{1}$$

and the equation of momentum conservation

$$\rho_0 \, \partial_t \mathbf{v} = -\mathbf{grad}(p), \tag{2}$$

yield the wave equation

$$\left(\Delta - \frac{1}{c^2}\partial_t^2\right) p = 0, \tag{3}$$

where $p$ denotes the acoustic pressure, $\mathbf{v}$ is the particle acoustic velocity, $\rho_0$ is the density of the air, and $c$ is the speed of the sound in the air. The boundary conditions will be specified in the following, for each particular case studied.

Because of the symmetry of the problem considered, $p$ and $\mathbf{v}$ only depend on the longitudinal and the transverse coordinates, noted $z$ and $r$ respectively. For this 2D-problem, the spatial operators are reduced to[12]

$$\mathrm{div}(\mathbf{v}) = \partial_z(\mathbf{v}.\mathbf{u_z}) + \frac{\mathbf{v}.\mathbf{u_r}}{r} + \partial_r(\mathbf{v}.\mathbf{u_r}), \tag{4}$$

$$\mathbf{grad}(p) = \partial_z p\, \mathbf{u_z} + \partial_r p\, \mathbf{u_r}, \tag{5}$$

and

$$\Delta p = \partial_z^2 p + \frac{1}{r}\partial_r p + \partial_r^2 p, \tag{6}$$

where $\mathbf{u_z}$ and $\mathbf{u_r}$ are the normal unitary vectors respectively associated with the coordinates $z$ and $r$, and "." denotes the scalar product.

## B. Perspective goals and description of the problem

Simulating the acoustic propagation in an axisymmetric waveguide requires solving the 2D-problem Eq. (3) with Eq. (6) for the boundary conditions on the wall as well as at the input and the output of the guide. For instance, target applications may require wall conditions such as motionless rigid walls (possibly with visco-thermal boundary layers) for models of wind instruments, or controlled moving and vibrating walls for vocal tract models. The purpose of this paper is to propose a method to derive models of such waveguides, which do not require a resolution in the 2D-inside space, allowing low-cost simulations (e.g. real-time applications). The idea developed in the following consists of reducing the 2D-problem to a 1D-complexity such as the Webster equation does, making assumptions as weak as possible.

The first step of the method is to separate the geometrical information carried by the time-varying isobaric maps from that of the propagation of the pressure travelling on it. This is done considering a change of coordinates $(z, r) = (f(s, u, t), g(s, u, t))$ where $s$ is chosen indexing isobars at each time (Sec. II B), defining $f$ and $g$ in an implicit way (Eq. (15)).

Thus, $z$ and $r$ become (like the pressure) dependent variables of the partial differential equation modelling the wave equation, and describe the isobaric map with respect to the independent variables $(s, u, t)$. Writing that $s$ indexes isobars (Eq. (15)) enables the derivation of the gradient of the pressure (Eq. (19)) and the wave equation (Eq. (20)) for $(s, u, t)$. This last equation exactly models the coupling of the propagation of the pressure with the isobaric map geometry, maps for which a necessary condition is straightforwardly deduced (Eq. (24)) and time-invariant specimens may be exhibited (Sec. II D).

As the pressure does not depend on $u$, having explicit expressions of the coefficients of the wave equation for a given $u$ suffice to furnish 1D-models. Choosing to describe the wall for a constant $u = w$ leads to an explicit parameterization $f|_w$, $g|_w$ of the wall (Eq. (31)). But this knowledge remains insufficient to isolate the propagation and the geometrical problems (Sec. III A) because of involved partial derivatives of $f$ and $g$ with respect to $u$, requiring a hypothesis.

The hypothesis of quasi-sphericity of isobars near the wall (Eq. (40)) makes the isolation of these problems possible. For lossless and motionless rigid walls, the deduced 1D-model (Eq. (42)) may be written for a $z$-description of the wall (Eq. (45)) or a $\ell$-description (Eq. (46)) which leads to a Webster equation, $\ell$ measuring the arc length of the wall. For more general wall conditions, the 1D-model (Eq. (58)) requires that isobars are nearly orthogonal to the wall (Sec. IV B) to preserve the linearity of the propagation with respect to the pressure. This is fulfilled for mobile walls in many practical cases and for motionless rigid walls which induce visco-thermal losses, leading to the respective models Eq. (67) and Eq. (71).

## II. DERIVATION OF EXACT EQUATIONS

This section establishes the wave equation in any coordinate system rectifying the isobaric map for axisymmetric problems. The calculations are exact as soon as isobaric maps may be locally described by a $\mathcal{C}^2$-regular diffeomorphism. Although topological aspects are not discussed here, a necessary geometrical condition is given for the map's admissibility. Before the method is described, various involved geometrical quantities are precisely defined for an arbitrary change of coordinates. The definitions and the notations of this preliminary part constitute the reference list of the geometrical quantities used in this paper.

### A. Geometrical definitions

Let $O$ and $\mathcal{B}^0 = (\mathbf{u_z}, \mathbf{u_r})$ be respectively the origin located on the axis of symmetry and the oriented canonical basis of the reference 2D-frame $(O, z, r)$. Let $\Phi$ be an arbitrary regular diffeomorphism defining a spatio-temporal change of coordinates $(s,u,t) = \Phi(z,r,t)$ which does not distort time. Then, the functions $f$ and $g$ defined by

$$z = f(s,u,t), \tag{7a}$$

$$r = g(s,u,t), \tag{7b}$$

exist and have the same regularity as $\Phi$. Such coordinates $s$ and $u$ are commonly called curvilinear because the variation of one of them does not make the corresponding point describe a straight line in the original space. The associated curves are noted, for each time $t$,

- $\mathcal{T}_{u,t}$ if $s$ varies and $u$ remains constant,
- $\mathcal{I}_{s,t}$ if $u$ varies and $s$ remains constant.

If $\Phi$ has a $\mathcal{C}^1$ regularity, a spatial local basis $\mathcal{B}_t$ for the $(s,u)$-coordinate system may be defined for each time $t$ by the vectors $\partial_s f \mathbf{u_z} + \partial_s g \mathbf{u_r}$ and $\partial_u f \mathbf{u_z} + \partial_u g \mathbf{u_r}$. Then are defined their respective norms $\sigma_s$ and $\sigma_u$, their associated unitary vectors $\mathbf{u_s}$ and $\mathbf{u_u}$, the characteristic oriented angles $\theta = (\mathbf{u_z}, \mathbf{u_s})$ and $\phi = (\mathbf{u_r}, \mathbf{u_u})$. These geometrical quantities represented in Fig. 1 are given by the following expressions:

$$\sigma_s = \sqrt{(\partial_s f)^2 + (\partial_s g)^2}, \tag{8a}$$

$$\sigma_u = \sqrt{(\partial_u f)^2 + (\partial_u g)^2}, \tag{8b}$$

$$\cos\theta = \partial_s f \,/\sigma_s, \tag{9a}$$

$$\sin\theta = \partial_s g \,/\sigma_s, \tag{9b}$$

$$\cos\phi = \partial_u g \,/\sigma_u, \tag{9c}$$

$$\sin\phi = -\partial_u f \,/\sigma_u, \tag{9d}$$

$$\mathbf{u_s} = \cos\theta\, \mathbf{u_z} + \sin\theta\, \mathbf{u_r}, \tag{10a}$$

$$\mathbf{u_u} = -\sin\phi\, \mathbf{u_z} + \cos\phi\, \mathbf{u_r}. \tag{10b}$$

For convenience, the vectors $\mathbf{u_s}$ and $\mathbf{u_u}$ rotated from the angle $+\frac{\pi}{2}$ are also introduced, namely:

$$\mathbf{w_s} = -\sin\theta\,\mathbf{u_z} + \cos\theta\,\mathbf{u_r}, \tag{11a}$$

$$\mathbf{w_u} = -\cos\phi\,\mathbf{u_z} - \sin\theta\,\mathbf{u_r}. \tag{11b}$$

[Figure 1 about here]

Then, the default of orthogonality of $\mathcal{B}_t$ can be exhibited by the angular deviation $\delta = (\mathbf{w_s}, \mathbf{u_u})$ and more generally by its tangent $\epsilon$ given by

$$\delta = \phi - \theta, \tag{12a}$$

$$\epsilon = \tan(\delta). \tag{12b}$$

Indeed, a local basis $\mathcal{B}_t$ is orthogonal if and only if $\epsilon = 0$. This is equivalent to the useful relation

$$\partial_s f \partial_u f + \partial_s g \partial_u g = 0. \tag{13}$$

Finally, the Mach numbers $\xi_s = \frac{1}{c}\mathbf{V}.\mathbf{u_s}$ and $\xi_n = \frac{1}{c}\mathbf{V}.\mathbf{w_s}$ respectively associated with the tangential and the normal components of the velocity $\mathbf{V}$ of a geometrical point (not that of the particle) located at $(s, u)$ are introduced. These dynamic quantities are given by

$$\xi_s = \frac{1}{c}[\partial_t f\,\cos\theta + \partial_t g\,\sin\theta], \tag{14a}$$

$$\xi_n = \frac{1}{c}[-\partial_t f\,\sin\theta + \partial_t g\,\cos\theta]. \tag{14b}$$

Note that a coordinate system compatible with the axial symmetry is such that

$$\forall u, t, \quad \exists u^* \,/\, \forall s, \left\{ \begin{array}{rcl} f(s, u^*, t) &=& f(s, u, t), \\ g(s, u^*, t) &=& -g(s, u, t). \end{array} \right.$$

This implies in particular that for each time, there exists $u_0$ such that $\mathcal{T}_{u_0,t}$ is the axis of symmetry. Generally, given an axisymmetric map $\{\mathcal{I}_{s,t}, \mathcal{T}_{u,t}\}$, a natural choice for its description consists of using $f$ and $g$ which have respectively an even and an odd $u$-parity.

### B. Rectification of the isobaric map

A change of coordinates $\Phi$ which rectifies the isobaric map is such that one ordinate indexes isobars while the other is not colinear to the first one to preserve $\Phi$ as a bijection. Confering the indexation of isobars to $s$ signifies that, for each time $t$, the curves $\mathcal{I}_{s,t}$ represent the isobars while the curves $\mathcal{T}_{u,t}$ are nowhere tangent to $\mathcal{I}_{s,t}$ (see Fig. 2).

`[Figure 2 about here]`

Thus, for any given $s$, the pressure does not depend on $u$, so the local rectification on a domain $\Omega$ is obtained for the condition

$$\exists \widetilde{p} \ / \ \forall (s,u,t) \in \Omega, \ \ p\left(f(s,u,t), g(s,u,t), t\right) = \widetilde{p}(s,t). \tag{15}$$

Assuming the $\mathcal{C}^2$ regularity for $f$, $g$, and $\widetilde{p}$, this implicit relation on $f$ and $g$ makes the derivation of the wave equation which governs $\widetilde{p}$ possible on $\Omega$. The method consists of signifying the link between the partial derivatives of $p(z,r,t)$ evaluated in $(z,r,t) = (f(s,u,t),\ g(s,u,t), t)$ and the partial derivatives of $\widetilde{p}(s,t)$, as described below.

Applying the differential operators $\partial_s$, $\partial_u$, and $\partial_t$ on Eq. (15) until the second order leads to the system

$$\widetilde{\mathcal{D}}(s,u,t) \ \ = \ \ \mathcal{M}(s,u,t) \ \ \mathcal{D}\left(f(s,u,t), g(s,u,t), t\right). \tag{16}$$

The corresponding explicit formulation is developped in Eq. (17), omitting to write the variables of evaluation for sake of compactness.

$$\underbrace{\begin{bmatrix} \partial_s \widetilde{p} \\ \partial_u \widetilde{p} \\ \partial_t \widetilde{p} \\ \partial_s^2 \widetilde{p} \\ \partial_u^2 \widetilde{p} \\ \partial_t^2 \widetilde{p} \\ \partial_s\partial_u \widetilde{p} \\ \partial_s\partial_t \widetilde{p} \\ \partial_u\partial_t \widetilde{p} \end{bmatrix}}_{\widetilde{\mathcal{D}}} = \underbrace{\begin{bmatrix} \partial_s f & \partial_s g & 0 & 0 & 0 & 0 & 0 & 0 & 0 \\ \partial_u f & \partial_u g & 0 & 0 & 0 & 0 & 0 & 0 & 0 \\ \partial_t f & \partial_t g & 1 & 0 & 0 & 0 & 0 & 0 & 0 \\ \partial_s^2 f & \partial_s^2 g & 0 & (\partial_s f)^2 & (\partial_s g)^2 & 0 & 2\,\partial_s f\,\partial_s g & 0 & 0 \\ \partial_u^2 f & \partial_u^2 g & 0 & (\partial_u f)^2 & (\partial_u g)^2 & 0 & 2\,\partial_u f\,\partial_u g & 0 & 0 \\ \partial_t^2 f & \partial_t^2 g & 0 & (\partial_t f)^2 & (\partial_t g)^2 & 1 & 2\,\partial_t f\,\partial_t g & 2\,\partial_t f & 2\,\partial_t g \\ \partial_s\partial_u f & \partial_s\partial_u g & 0 & \partial_s f\,\partial_u f & \partial_s g\,\partial_u g & 0 & \begin{matrix}\partial_s f\,\partial_u g \\ +\partial_u f\,\partial_s g\end{matrix} & 0 & 0 \\ \partial_s\partial_t f & \partial_s\partial_t g & 0 & \partial_s f\,\partial_t f & \partial_s g\,\partial_t g & 0 & \begin{matrix}\partial_s f\,\partial_t g \\ +\partial_t f\,\partial_s g\end{matrix} & \partial_s f & \partial_s g \\ \partial_u\partial_t f & \partial_u\partial_t g & 0 & \partial_u f\,\partial_t f & \partial_u g\,\partial_t g & 0 & \begin{matrix}\partial_u f\,\partial_t g \\ +\partial_t f\,\partial_u g\end{matrix} & \partial_u f & \partial_u g \end{bmatrix}}_{\mathcal{M}} \underbrace{\begin{bmatrix} \partial_z p \\ \partial_r p \\ \partial_t p \\ \partial_z^2 p \\ \partial_r^2 p \\ \partial_t^2 p \\ \partial_z\partial_r p \\ \partial_z\partial_t p \\ \partial_r\partial_t p \end{bmatrix}}_{\mathcal{D}}, \quad (17)$$

Then, $\mathcal{D}$ is formally obtained from Eq. (16) by computing $\mathcal{M}^{-1}\widetilde{\mathcal{D}}$ and remarking that

$$\widetilde{\mathcal{D}}^T = [\partial_s\widetilde{p},\ 0,\ \partial_t\widetilde{p},\ \partial_s^2\widetilde{p},\ 0,\ \partial_t^2\widetilde{p},\ 0,\ \partial_s\partial_t\widetilde{p},\ 0], \tag{18}$$

since $\partial_u\widetilde{p}(s,t) = 0$. Expressions signified with the mono-space dependent pressure $\widetilde{p}(s,t)$ are straightforwardly deduced for the gradient from Eq. (5) and for the wave equation from Eq. (3) and Eq. (6) evaluated in $(z,r,t) = (f(s,u,t), g(s,u,t), t)$. After simplification and using the notations defined in II A, these relations may be written

$$\mathbf{grad}(\widetilde{p}) = \frac{\partial_s\widetilde{p}}{\sigma_s}[\mathbf{u_s} + \epsilon\,\mathbf{w_s}], \tag{19}$$

and

$$A_{s,s}\partial_s^2\widetilde{p} + A_s\partial_s\widetilde{p} + A_{s,t}\partial_s\partial_t\widetilde{p} - \frac{1}{c^2}\partial_t^2\widetilde{p} = 0, \tag{20}$$

where the coefficients given by

$$\begin{aligned}
A_{s,s} &= \frac{1+\epsilon^2-(\xi_s+\epsilon\xi_n)^2}{\sigma_s^2}, && \text{(21a)}\\
A_s &= \frac{\sin\theta+\epsilon\cos\theta}{g\,\sigma_s} + \frac{1-\xi_n^2}{\sigma_s^2}\Bigg[\partial_s(\epsilon^2) \\
&\quad +(1+\epsilon^2)\left(\frac{\sigma_s\partial_u\phi}{\sigma_u\cos\delta}+\epsilon\partial_s\theta-\partial_s\ln\sigma_s\right)\Bigg] \\
&\quad -\frac{1}{2}\partial_s\left(\frac{\xi_s^2+2\epsilon\xi_s\xi_n-\xi_n^2}{\sigma_s^2}\right) - \frac{\xi_s\xi_n}{\sigma_s^2}\partial_s\epsilon \\
&\quad +\frac{1}{c}\partial_t\left(\frac{\xi_s+\epsilon\xi_n}{\sigma_s}\right) + \frac{\xi_n}{c\,\sigma_s}\partial_t\epsilon, && \text{(21b)}\\
A_{s,t} &= 2\,\frac{\xi_s+\epsilon\xi_n}{c\,\sigma_s}, && \text{(21c)}
\end{aligned}$$

are expressions of $f$ and $g$ exclusively and depend on $(s,u,t)$. Although the tedious calculations are not detailed, note that this process cannot be reduced to writing the Laplacian operator for the change of coordinates $\Phi$, as for usual static coordinates. Thus, the Mach numbers $\xi_s$ and $\xi_n$ involved in Eqs. (21) are precisely the contribution of the term $\partial_t^2 p$ in Eq. (3). They are the expression of the dynamic of the isobaric map.

Note that choosing $u$ such that $\mathcal{T}_{u,t}$ represent the field lines leads without loss of generality to simpler expressions for which $\epsilon=0$ because of the orthogonality of $\mathcal{I}_{s,t}$ and $\mathcal{T}_{u,t}$ at each point. This concise formulation is exploited in Sec. II D to exhibit time-invariant isobaric maps, and in Sec. III to derive a mono-space dependent wave equation for motionless rigid walls. Whereas, the study dealing with mobile walls having small admittances presented in Sec. IV requires being driven with non orthogonal coordinates so that Eq. (20) is established in this more general context.

A remarkable property of these equations is that they are not modified by any bijective regular change of variables such that $s=\alpha(\hat{s},\hat{t})$, $u=\beta(\hat{s},\hat{u},\hat{t})$, and $t=\hat{t}$: taking $\hat{s}$, $\hat{u}$, $\hat{t}$, $\hat{f}(\hat{s},\hat{u},\hat{t})=f(\alpha(\hat{s},\hat{t}),\beta(\hat{s},\hat{u},\hat{t}),\hat{t})$, $\hat{g}(\hat{s},\hat{u},\hat{t})=g(\alpha(\hat{s},\hat{t}),\beta(\hat{s},\hat{u},\hat{t}),\hat{t})$, and $\hat{p}(\hat{s},\hat{t})=\widetilde{p}(\alpha(\hat{s},\hat{t}),\hat{t})$, in place of $s$, $u$, $t$, $f$, $g$, and $\widetilde{p}$ keeps the formula identical. Moreover, the axial symmetry is also naturally supported by the isobaric wave equation. Indeed, for $f$ and $g$ having respectively an even and an odd $u$-parity, applying $u\mapsto -u$ on Eq. (20) leaves this equation invariant.

### C. Regular isobaric maps and admissibility

A necessary condition, An admissibility condition for isobaric maps, which is independent of the pressure, may be deduced from Eq. (20) on $(f, g)$. This criterion of admissibility furnishes a property inherent to the set of regular isobaric maps. It proves in particular that any arbitrary regular map does not always match with a wave propagation phenomenon.

The derivation of this condition relies on the $u$-independence of $\widetilde{p}$. The method consists of applying operators $\partial_u^k$ on Eq. (20). As the factors represented by $\mathcal{P} = \left[\partial_s^2\widetilde{p}\ \partial_s\widetilde{p}\ \partial_s\partial_t\widetilde{p}\ \partial_t^2\widetilde{p}\right]^T$, do not depend on $u$, they may be eliminated by making linear combinations of four distinct relations proceeding from four distinct integers $k$. In fact, only three of these relations suffice as the proof below describes it.

As soon as the $\mathcal{C}^2$ functions $f$ and $g$ have in addition a $\mathcal{C}^5$-regularity for the variable $u$, the operators $\partial_u^k$ $(k = 0, 1, 2, 3)$ applied on Eq. (20) yields to the system

$$\mathcal{A}\,\mathcal{P} = \mathbf{0}, \tag{22}$$

where

$$\mathcal{A} = \begin{bmatrix} A_{s,s} & A_s & A_{s,t} & -\frac{1}{c^2} \\ \partial_u A_{s,s} & \partial_u A_s & \partial_u A_{s,t} & 0 \\ \partial_u^2 A_{s,s} & \partial_u^2 A_s & \partial_u^2 A_{s,t} & 0 \\ \partial_u^3 A_{s,s} & \partial_u^3 A_s & \partial_u^3 A_{s,t} & 0 \end{bmatrix}. \tag{23}$$

For a propagative phenomenon $\mathcal{P} \neq \mathbf{0}$. $\mathcal{P}$ is then an eigenvector of $\mathcal{A}$ associated with the eigenvalue 0. This proves that $\det(\mathcal{A}) = 0$. By developing the determinant with respect to the last column, a simpler equivalent formulation is obtained for

$$\det \begin{bmatrix} \partial_u A_{s,s} & \partial_u A_s & \partial_u A_{s,t} \\ \partial_u^2 A_{s,s} & \partial_u^2 A_s & \partial_u^2 A_{s,t} \\ \partial_u^3 A_{s,s} & \partial_u^3 A_s & \partial_u^3 A_{s,t} \end{bmatrix} = 0. \tag{24}$$

This necessary condition only involves the equations derived for $k = 1, 2, 3$. Equation (24) closes the proof since $A_{s,s}$, $A_s$, and $A_{s,t}$ only depend on $f$ and $g$, and thus, on the dynamic geometry.

The criterion Eq. (24) can be straighforwardly computed for any given maps to check their admissibility. But, practically, exhibiting analytical descriptions of admissible isobaric maps from it becomes unreachable as soon as the requisite dynamic and geometrical properties are not trivial.

### D. Globally time-invariant isobaric maps

This section presents an investigation on the restricted case of globally time-invariant maps on which propagative waves may travel. In order to exhibit only the physical propagative solutions, the pressure is assumed to be such that the functions $\partial_s^2\widetilde{p}$, $\partial_s\widetilde{p}$, and $\partial_t^2\widetilde{p}$ are non zero and real. The investigation is run directly from the isobaric wave equation rather than the admissibility criterion which only gives a necessary condition.

A globally time-invariant map may be described by time-independent functions $f(s,u)$ and $g(s,u)$. Choosing $\mathcal{T}_u$ as the field lines yields the constraint $\epsilon = 0$. Thus, the solution maps may be represented without loss of generality by $(f,g)$ satisfying Eq. (13) and

$$\partial_s^2\widetilde{p} + \partial_s\mathcal{L}\;\partial_s\widetilde{p} - \frac{\sigma_s^2}{c^2}\,\partial_t^2\widetilde{p} = 0, \tag{25}$$

calculated from Eq. (20) multiplied by $\sigma_s^2$. $\mathcal{L}$ is given by

$$\mathcal{L} = \ln\left|g\,\frac{\sigma_u}{\sigma_s}\right|, \tag{26}$$

remarking that Eq. (13) implies $\partial_u\phi/\cos^3\delta = \partial_u\theta = \partial_s\sigma_u/\sigma_s$. Then, two cases appear.

#### 1. $\sigma_s$ does not depend on $u$

In this case, $\partial_s\mathcal{L}$ does not depend on $u$ either (see Eq. (25)). Parallel planes orthogonal to $(Oz)$ and coaxial cylinders are obtained for $\partial_s g = 0$ and $\partial_u g = 0$ respectively. Except for these pathological cases, Eq. (13) ensures that $\partial_s f$, $\partial_u f$, $\partial_s g$, and $\partial_u g$ are non zero.

Then, Eq. (13) makes the elimination of $\partial_s f$ possible in $\partial_u(\sigma_s^2) = 0$ calculated from the definition Eq. (8a). The result $\partial_s \ln|\partial_u g| = \partial_s \ln|\partial_u f|$ equivalent to $\partial_s \ln|\tan\phi| = 0$ (see Eq. (9c) and Eq. (9d)) proves that $\phi$ only depends on $u$. As $\epsilon = \tan(\phi-\theta)$ is zero, $\theta$ is an exclusive function of $u$ as well. Equations (9a) and (9b) show that

$$\begin{aligned} f(s,u) &= R(s)\cos\theta(u) + F(u), && (27a)\\ g(s,u) &= R(s)\sin\theta(u) + G(u), && (27b)\end{aligned}$$

where $R' = \sigma_s$, and $F$ and $G$ are arbitrary.

Now, from Eq. (9c), $\sigma_u = \partial_u g/cos\phi$ so that $\partial_s\partial_u\mathcal{L} = 0$ can be written $\partial_u\partial_s \ln|g\partial_u g| = 0$ which, with Eq. (27b), leads to

$$G(u) = R_0 \sin\theta(u),$$

$R_0$ being an arbitrary constant. Finally, the calculation of Eq. (13) using Eqs. (27) with this function $G$ yields

$$F(u) = R_0 \cos\theta(u) + F_0,$$

where $F_0$ is arbitrary. The corresponding isobars are concentric spheres. This conclusion completes the proof that parallel planes, coaxial cylinders, and concentric spheres are the only regular globally time-invariant isobaric maps for which $\sigma_s$ does not depend on $u$.

### 2. $\sigma_s$ depends on $u$

In this case, $\partial_s\mathcal{L}$ also depends on $u$. Applying $\partial_u$ to Eq. (25) leads to

$$\partial_u\partial_s\mathcal{L}\ \partial_s\widetilde{p} - \frac{\partial_u\left(\sigma_s^2\right)}{c^2}\,\partial_t^2\widetilde{p} = 0.$$

Since $\partial_u\sigma_s$ and $\partial_s\widetilde{p}$ are assumed non zero, this relation proves that $\partial_t^2\widetilde{p}/\partial_s\widetilde{p}$ does not depend on $t$. Then, Eq. (25) proves that $\partial_s^2\widetilde{p}/\partial_s\widetilde{p} = \partial_s \ln|\widetilde{p}|$ does not depend on $t$ either, so that a general solution is $\widetilde{p}(s,t) = A(s)\,b(t) + C(t)$ where $A$, $b$, and $C$ are real functions. Writing Eq. (25) for this solution and applying the operator $X \mapsto \partial_t(X/b(t))$ on it show that both $b''(t)/b(t) = \mu^2$ and $C''(t)/b(t) = c_0$ are real constants so that $C(t) = c_0 b(t) + c_1 t + c_2$ with $(c_1, c_2) \in \mathbb{R}^2$. Defining $a(s) = A(s) + c_0$, this proves that the general solution is

$$\widetilde{p}(s,t) = a(s)b(t) + c_1 t + c_0,$$

with

$$b(t) = b_1 e^{\mu t} + b_2 e^{-\mu t}.$$

where $b_1$, $b_2$ are complex arbitrary constants such that $b(t)$ is real. Although it does not affect the following, note that physical cases requires that $c_1 = c_0 = 0$ since $\widetilde{p}$ is the acoustic pressure.

Using Eq. (26), Eq. (25) may be then reduced to

$$\frac{a'}{\sigma_s^2}\partial_s \ln\left|\frac{a'}{\sigma_s} g\,\sigma_u\right| = \frac{\mu^2}{c^2}.$$

Moreover, if the spatial dependence $a$ for the mode $\mu$ is locally bijective, posing $\hat{s} = a(s)$, and then defining $\hat{f}(\hat{s}, u, t) = f(s, u, t)$ and $\hat{g}(\hat{s}, u, t) = g(s, u, t)$ yields

$$\frac{1}{\hat{\sigma}_{\hat{s}}^2}\partial_{\hat{s}} \ln \left| \frac{\hat{g}\,\hat{\sigma}_{\hat{s}}}{\hat{\sigma}_u} \right| = \frac{\mu^2}{c^2}. \tag{28}$$

This equation shows that if a time-invariant isobaric map for which $\sigma_s$ depends on $u$ exists, this map necessarily depends on a mode $\mu$ corresponding to a pure frequency ($\mu$ imaginary) or a pure exponential ($\mu$ real). More precisely, once given the geometry of the wall parameterized with $s, u$ and expressing the boundary conditions, Eq. (28) gives the isobaric map associated with the mode $\mu$.

Finally, parallel planes, coaxial cylinders, and concentric spheres are the general time-invariant isobaric maps. This corroborates the Putland's results which exhibited them as those making the separation of variables possible. However, other singular maps for which the coefficients of the isobaric wave equation depend on both $s$ and $u$ may exist. They are necessarily associated with a mode $\mu$. This last case would correspond to have the wronskian defined by Putland[8] being zero (see Eqs. (19),(20) in his paper).

## III. MONO-SPACE DEPENDENT WAVE EQUATION FOR LOSSLESS AND MOTIONLESS RIGID WALLS

A rigorous derivation of a mono-space model of a waveguide proves to be unworkable for arbitrary geometries. Even if the exact equation (20) governs a mono-space dependent pressure, signifying $A_{s,s}$, $A_s$, and $A_{s,t}$ as well as possible from the shape of the waveguide does not succeed in such a 1D-model, as described below.

### A. Problem posed by the derivation of a 1D-model

Let $\Phi$ be now a particular local change of coordinates such that the wall noted $\mathcal{W}_t$ is simply described for a fixed $u$ noted $w$ so that

$$\mathcal{T}_{w,t} = \mathcal{W}_t. \tag{29}$$

This can be achieved as soon as $\mathcal{W}_t$ is not tangent to isobars, what is discussed below. Adopting the notation

$$q|_w(s,t) = q(s,w,t), \tag{30}$$

to indicate that a quantity $q(s,u,t)$ is evaluated on the wall $\mathcal{W}_t$, the profile of $\mathcal{W}_t$ is parameterized by

$$z = f|_w(s,t), \tag{31a}$$

$$r = g|_w(s,t). \tag{31b}$$

Then, once given a wall parameterization $(f|_w, g|_w)$, signifying the coefficients from the wall geometry simply consists of evaluating them on $\mathcal{W}_t$, namely imposing $u = w$. But, as conceivable, this process makes a difficulty stand out which clarifies why decoupling the propagation problem and the geometry of isobars is generally impossible.

This section exhibits the problem for walls assumed ideally rigid, lossless, and motionless: $\mathcal{T}_{w,t} = \mathcal{W}_t = \mathcal{W}$ so that $f|_w$ and $g|_w$ can be chosen time-independent and $\xi_s|_w = \xi_n|_w = 0$ (see Eq. (14)). In this case, the corresponding boundary condition is that the particle velocity $\mathbf{v}$, and so from Eq. (2), the gradient of the pressure $\mathbf{grad}(p)$, have no component normal to the wall. For locally non-degenerated cases ($\mathbf{grad}(p) \neq \mathbf{0}$), isobars are necessarily orthogonal to the wall $\mathcal{W}$. Considering a domain $\Omega$ on which this condition is satisfied, this proves that $\mathcal{W}$ belongs to the field lines so that $\epsilon|_w = 0$ (see Eq. (12b)). Note that if the gradient is zero on a set of isolated points, local solutions of the same 1D-model can be concatenated to form a maximal solution under the $\mathcal{C}^2$-regularity assumption. If this set has a non zero measure, the pressure computed from a mono-space partial differential equation of finite order is necessarily locally constant for both the time and the space variables. On this set, the partial derivatives of the pressure are zero and will make the 1D-linear model locally trivial $(0 = 0)$, independently of the involved coefficients. Practically, these properties makes it possible to proceed considering the only case $\epsilon|_w = 0$, without loss of generality.

Now, $\epsilon|_w = 0$ and $\xi_s|_w = \xi_n|_w = 0$ yields, for $u = w$, the simplified coefficients $A_{s,s} = 1/\sigma_s^2$, $A_{s,t} = 0$, and using Eq. (9b), $A_s = \partial_s \ln(g/\sigma_s)/\sigma_s^2 + \partial_u \phi/(\sigma_s \sigma_u \cos\delta)$.

As $f|_w$ and $g|_w$ may be derived with respect to $s$, they make the evaluation of $\sigma_s$ and $\partial_s \ln(g/\sigma_s)$ for $u = w$ possible, using Eq. (8a). On the contrary, they cannot give information on $\partial_u f|_w$ and $\partial_u g|_w$ and Eq. (13) yields only a relation beween them and $|\cos\delta| = 1$. because of their evaluation for $u = w$. Finally, the quantity $\partial_u \phi/(\sigma_u \cos\delta)$ included in $A_s$ cannot be evaluated for $u = w$ from $f|_w$, $g|_w$, and using $\epsilon|_w = 0$.

To cope with this difficulty, a local geometrical hypothesis is presented, which gives a natural extension of the exact models of propagation in tubes and cones.

### B. Geometrical hypothesis

Let $M(s)$ be a point of $\mathcal{W}$ indexed by $s$. Let $\mathcal{S}_s$ be the sphere tangent to $\mathcal{I}_{s,t}$ in $M(s)$ and centered in $O_s \in (Oz)$ (see Fig. 3). Then are defined the z-ordinate $z_{O_s}(s)$ of $O_s$, the radius $R_s(s)$ of the sphere $\mathcal{S}_s$, and for any point $N(s,u,t)$, the distance $r_{\mathcal{I}}(s,u,t)$ between $O_s$ and $N$.

`[Figure 3 about here]`

By definition, the radius $\mathbf{O_s M}$ is orthogonal to the sphere $\mathcal{S}_s$ and so to $\mathbf{u_u}$ in $M(s)$. Writing that the scalar product of $\mathbf{O_s M}$ and $\mathbf{u_u}$ is zero, $z_{O_s}(s)$ is proven to be such that

$$g|_w = \tan\phi|_w \, \left(f|_w - z_{O_s}\right). \tag{32}$$

The positive radii $R_s(s)$ and $r_{\mathcal{I}}(s,u,t)$ are given by

$$R_s{}^2 = \left.\frac{g^2}{\sin^2\theta}\right|_w = \left.\frac{g^2}{\sin^2\phi}\right|_w, \tag{33a}$$

$$r_{\mathcal{I}}{}^2 = g^2 + (f - z_{O_s})^2. \tag{33b}$$

The relative divergence $\varsigma(s,u,t)$ is then introduced by

$$\varsigma = \frac{r_{\mathcal{I}}}{R_s} - 1. \tag{34}$$

$\varsigma$ may be interpreted as an indicator of the deformation engendering $\mathcal{I}_{s,t}$ from $\mathcal{S}_s$. Note that if the wall $\mathcal{W}$ is locally parallel to $(Oz)$, $\varsigma$ may keep a meaning by continuation, although $R_s$ becomes infinite. In particular, the study below proves that $\varsigma|_w$ is zero at the first order at least.

By definition, $r_{\mathcal{I}}(s,w,t) = R_s(s)$ so that

$$\varsigma|_w = 0. \tag{35}$$

Now, $\partial_u\varsigma = \partial_u\left(r_{\mathcal{I}}{}^2\right) / \left(2 r_{\mathcal{I}} R_s\right)$. From Eq. (33b), Eq. (9c), and Eq. (9d)

$$\frac{1}{2}\partial_u\left(r_{\mathcal{I}}{}^2\right) = \sigma_u\left[g\cos\phi - (f - z_{O_s})\right]. \tag{36}$$

The definition of $z_{O_s}$ shows that Eq. (36) is zero for $u = w$ so that

$$\left(\partial_u\varsigma\right)|_w = 0. \tag{37}$$

Note that, in fact, this last equation is related to the tangency of $\mathcal{S}_s$ and $\mathcal{I}_{s,t}$ in $M(s)$. Finally,

$$\partial_u^2 \varsigma = \frac{\partial_u^2 \left(r_{\mathcal{I}}{}^2\right)}{2 r_{\mathcal{I}} R_s} - \frac{\left(\partial_u \left(r_{\mathcal{I}}{}^2\right)\right)^2}{2 r_{\mathcal{I}}{}^2 R_s},$$

so that the second term is zero in $u = w$ (see Eq. (36)), and

$$\begin{aligned} \frac{1}{2}\partial_u^2 \left(r_{\mathcal{I}}{}^2\right) &= \partial_u \sigma_u \left[\cos\phi - (f - z_{O_s}) \sin\phi\right] + \sigma_u^2 \\ &\quad - \sigma_u \partial_u \phi \left[g \sin\phi + (f - z_{O_s}) \cos\phi\right], \end{aligned} \tag{38}$$

for which the first term is zero in $u = w$. Then, $\left(\partial_u^2 \varsigma\right)\big|_w$ is given by

$$\left(\partial_u^2 \varsigma\right)\Big|_w = \left[\frac{\sigma_u}{R_s{}^2}\left(\sigma_u - \frac{g\,\partial_u \phi}{\sin\phi}\right)\right]\Bigg|_w . \tag{39}$$

The geometrical hypothesis proposed in this section consists of assuming that near the wall $\mathcal{W}$, isobars $\mathcal{I}_{s,t}$ deviate from $\mathcal{S}_s$ "slower than a parabola", namely:

$$\left(\partial_u^2 \varsigma\right)\Big|_w = 0. \tag{40}$$

As $\sigma_u / R_s{}^2 \neq 0$, this hypothesis yields

$$\left.\frac{\partial_u \phi}{\sigma_u}\right|_{s,w,t} = \left.\frac{\sin\phi}{g}\right|_{s,w,t}, \tag{41}$$

which will make the evaluation of $A_s|_w$, and so of Eq. (20) on $\mathcal{W}$, possibly signified with $f|_w$ and $g|_w$.

## C. Mono-space wave equation

As $\epsilon|_w = 0$, $\sin\phi / \cos\delta = \sin\theta = \partial_s g / \sigma_s$ for $u = w$. The geometrical hypothesis and this last equation make the evaluation of $A_s|_w$ possible. Finally, recalling that $\xi_s|_w = \xi_n|_w = 0$, this leads to the significantly simplified equation

$$A_{s,s}|_w \partial_s^2 \widetilde{p} + A_s|_w \partial_s \widetilde{p} - \frac{1}{c^2} \partial_t^2 \widetilde{p} = 0, \tag{42}$$

where $A_{s,s}|_w$ and $A_s|_w$ are given by

$$A_{s,s}|_w = \left.\frac{1}{\sigma_s^2}\right|_w, \tag{43a}$$

$$A_s|_w = \left.\frac{2\partial_s \ln g}{\sigma_s^2}\right|_w . \tag{43b}$$

Furthermore, because $\epsilon|_w = 0$, Eq. (19) leads to

$$\mathbf{grad}(\widetilde{p}) = \frac{\partial_s \widetilde{p}}{\sigma_s}\mathbf{u_s}, \tag{44}$$

on $\mathcal{W}$.

The obtained 1D-model is available for any choice made for $s$, all the deduced models being equivalent. This modelling is now established for two particular and natural parameterizations. The first one consists of choosing $s = z$ so that $g|_w(s) = R(s)$ represents the radius $R(z)$ of the section of the waveguide located by the $z$-ordinate $z = f|_w(s) = s$. In this case, $\sigma_s(z, w, t) = \sqrt{1 + R'(z)^2}$ leading to

$$\partial_z^2 \widetilde{p}(z,t) + 2\frac{R'(z)}{R(z)}\partial_z \widetilde{p}(z,t) - \frac{1 + R'(z)^2}{c^2}\partial_t^2 \widetilde{p}(z,t) = 0. \tag{45}$$

Note that this equation does not model the propagation of the lowest mode since it differs from that established by Pagneux[10] (Eq. (45)) when higher-orders modes are ignored.

The second choice is to take $s = \ell$ where $\ell$ represents the arc length of the curve $\mathcal{C}_\ell \subset \mathcal{W}$ starting from a reference point $M(0)$ and stopping at the considered point $M(s)$. This ordinate $\ell$ is such that $\sigma_s|_w = 1$. Noting $\mathcal{R}(\ell)$ the radius of the section of the waveguide located by $\ell$, the obtained wave equation is that of Webster:

$$\partial_\ell^2 \widetilde{p}(\ell,t) + 2\frac{\mathcal{R}'(\ell)}{\mathcal{R}(\ell)}\partial_\ell \widetilde{p}(\ell,t) - \frac{1}{c^2}\partial_t^2 \widetilde{p}(\ell,t) = 0. \tag{46}$$

This result makes it possible to attribute all the known properties of this equation to the general model Eq. (42), such as the conservation of the acoustical energy, or the existence of analytical solutions for particular profiles. For this reason, this equation is the one which is used in the following rather than Eq. (42) or Eq. (45).

## D. Observations and discussion

As a first result, the hypothesis of quasi-sphericity Eq. (41) makes the arc length $\ell$ appear as the natural longitudinal ordinate for the 1D-model. This exactly coincides with the ordinate for which Putland establishes the Webster equation. However, the coefficients ahead of $\partial_\ell \widetilde{p}$ are distinct for both models. That of Putland is $\partial_\ell S(\ell,t)/S(\ell,t)$ where $S$ denotes the area of the isobaric (or the "$\ell$-iso") surfaces[8] versus $2\mathcal{R}'/\mathcal{R}$ for Eq. (46) which is time-invariant. Considering $2\mathcal{R}'/\mathcal{R}$ as a ratio $S'(\ell)/S(\ell)$, where $S$ would represent the plane section of the waveguide drawn for $\ell$ but not $z$, yields a similar formulation but remains physically distinct.

Moreover, this model holds various remarkable properties. First of all, it gives exact results for both straight and conical pipes. Thus, for a straight pipe defined by $R(z) = R_0$, and a conical pipe defined by $R(z) = z \tan\theta_0$ or $\mathcal{R}(\ell) = \ell \sin\theta_0$ (see Eq. (52)) with $\theta_0 \in ]0, \pi/2[$, the 1D-modelling leads to, respectively,

$$\partial_z^2 \widetilde{p}(z,t) - \frac{1}{c^2}\partial_t^2 \widetilde{p}(z,t) = 0, \tag{47a}$$

$$\partial_\ell^2 \widetilde{p}(\ell,t) + \frac{2}{\ell}\partial_\ell \widetilde{p}(\ell,t) - \frac{1}{c^2}\partial_t^2 \widetilde{p}(\ell,t) = 0. \tag{47b}$$

As expected, Eq. (47a) and Eq. (47b) yield the exact models for plane waves and spherical waves.

Compared to the Webster equations established assuming plane, spherical, or oblate spheroidal wavefronts, sensible improvements of the presented model may be highlighted. The orthogonality between isobars and the wall is not only respected, but the unavoidable mobility of isobars (see Sec. II D) is respected too. As a matter of fact, this is a consequence of the locality as well as the minimal order of the hypothesis which only requires $\partial_u^2 \varsigma|_w = 0$ while $\varsigma|_w$ and $\partial_u \varsigma|_w$ are both naturally zero.

Unfortunately, most of the limitations known for the Webster equation remain. The validity of the geometrical hypothesis and, therefore, of the model is restricted to a low frequency range and smooth geometries so that high mode coupling may not occur[10]. Walls may have a small curvature as well as isobars.

In particular, the model does not make the control of the geometry of isobars possible either at the input or at the output of the pipe: spheres appear as the best appropriate shapes for the quasi-sphericity hypothesis. Rigorously, these input-ouput geometries should be exhibited by solving Eq. (20) for $(f, g)$ and knowing $(f|_w, g|_w)$, once the pressure $\widetilde{p}(s,t)$ has been computed for the 1D-model and for the 1D-boundary conditions. Note that, practically, the geometrical resolution could be driven with numerical methods and for the simplifying assumption $\epsilon = 0$, leading to a description of the isobaric maps by time varying orthogonal coordinate systems. But since 1D-models are generally not exact, the pressure established for any of them should be linked to "aberrant maps" (unsolvable or not axisymmetric). The prospect of deriving a 1D-modelling from Eq. (20) for new more relaxed geometrical hypotheses and making a control possible on the boundary isobars will be opened up in the conclusion.

### E. Particular profiles

Analytical solutions of the Webster equation are known for particular shapes defined by (for strictly positive $R_0$ and $\ell_0$)

**(i)** $\mathcal{R}(\ell) = R_0 \exp(\alpha\ell)$ (exponential),

**(ii)** $\mathcal{R}(\ell) = R_0 \cosh(\alpha\ell)$ (catenoidal),

**(iii)** $\mathcal{R}(\ell) = R_0 \sin(\alpha\ell)$ (sinusoidal),

**(iv)** $\mathcal{R}(\ell) = R_0 \ell^\alpha$ (Bessel).

Indeed, noting $\psi(\ell,\omega)$ the Fourier transform of $\mathcal{R}(\ell)\,\widetilde{p}(\ell,t)$ where $\omega$ denotes the time pulsation, the wave equation corresponding to the cases **(i-iii)** is obtained for

$$\partial_\ell^2 \psi(\ell,\omega) - \left(\Upsilon - \frac{\omega^2}{c^2}\right)\psi(\ell,\omega) = 0, \tag{48}$$

where $\Upsilon = \mathcal{R}''(\ell)/\mathcal{R}(\ell)$ is constant. The solutions in the Fourier domain are then

$$\psi(\ell,\omega) = \psi_0(\omega)\,\mathrm{e}^{r(\omega)\ell} + \psi_1(\omega)\,\mathrm{e}^{-r(\omega)\ell}, \tag{49}$$

where $r(\omega)$ is a square root of $\Upsilon - (\omega/c)^2$ and $\psi_0$, $\psi_1$ are arbitrary. When $\Upsilon > 0$, a cut-off pulsation $\omega_c = c\sqrt{\Upsilon}$ may be defined: $r(\omega)$ is imaginary and the corresponding wave is propagative only for $\omega \geq \omega_c$. Note that although this equation is usually written in this form, Berners[13] has shown that the travelling modes which constitutes the Fourier basis set do not furnish a complete set for convex profiles ($\Upsilon < 0$). In this case, the set of eigenfunctions of the associated Sturm-Liouville problem may include the so-called "trapped modes". This requires to consider Eq. (48) in the Laplace domain rather than that of Fourier.

For the Bessel horns **(iv)**, noting $P(\ell,\omega)$ the Fourier transform of $\widetilde{p}(\ell,t)$, the corresponding wave equation is

$$\partial_\ell^2 P(\ell,\omega) + \frac{2\alpha}{\ell}\partial_\ell P(\ell,\omega) + \frac{\omega^2}{c^2}P(\ell,\omega) = 0, \tag{50}$$

so that solutions take the form

$$P(\ell,\omega) = P_0(\omega)\,\ell^{\frac{1}{2}-\alpha}\,J_{\alpha-\frac{1}{2}}\!\left(\frac{\ell\omega}{c}\right) + P_1(\omega)\,\ell^{\frac{1}{2}-\alpha}\,Y_{\alpha-\frac{1}{2}}\!\left(\frac{\ell\omega}{c}\right) \tag{51}$$

where $J_\nu$ and $Y_\nu$ are the Bessel functions of, respectively, the first kind and the second kind[14] (chapter 9), and $P_0$, $P_1$ are arbitrary.

Nevertheless, such profiles are known when the Webster equation is written for the variable $z$ rather than $\ell$. Thus, although analytical results are unchanged for the pressure resolution, that is not the case for the real physical shapes. In particular, the new computed profiles have an unusual characteristic: their radius or their length may be required to be bounded.

### 1. Properties of physical shapes

Let $z \mapsto L(z)$ be the positive length of the wall $\mathcal{W}$ from $z_0$ to $z > z_0$. Then, $\mathrm{d}L = \sqrt{1+R'(z)^2}\,\mathrm{d}z$. Deriving the expression $R(z) = \mathcal{R}(L(z))$ gives

$$\mathcal{R}'(L(z)) = \frac{R'(z)}{\sqrt{1+R'(z)^2}}. \tag{52}$$

This implies that $|\mathcal{R}'| \leq 1$, the limit case $|\mathcal{R}'| = 1$ corresponding to an infinite slope for the physical shape. Except for the sinusoidal profile when $|\alpha R_0| < 1$, the formula $\mathcal{R}(\ell)$ remains physically meaningful only on lower or upper bounded intervals so that a maximum or minimum radius $R^*$ associated with a length $\ell^*$ may be defined (see Table (II)).

Note that if a $\mathcal{C}^1$-regular profile ends with a slope $\mathcal{R}' = 1$ at $\ell = \ell^*$, prolonging the profile by the cone such that $\forall \ell \geq \ell^*$, $\mathcal{R}'(\ell) = 1$ corresponds to model the pipe baffled. This profile still satisfies the $\mathcal{C}^1$-regularity. In this case, Eq. (46) proves that, for $\ell \geq \ell^*$, the pressure propagates as spherical waves.

### 2. Computation of physical shapes

The computation of $R(z)$ from $\mathcal{R}(\ell)$ can be achieved in an implicit way if there exists $F$ such that $\mathcal{R}' = F(\mathcal{R})$. In this case, Eq. (52) yields $\frac{R'(z)}{\sqrt{1+R'(z)^2}} = F(\mathcal{R}(L(z))) = F(R(z))$ which is proven equivalent to

$$\frac{F(R(z))}{\sqrt{1-F(R(z))^2}}\,R'(z) = 1. \tag{53}$$

If $z \mapsto F(R(z)) \,/\, \sqrt{1-F(R(z))^2}$ is bijective, the integration of Eq. (53) from $z_0$ to $z$ may be written

$$\int_{R(z_0)}^{R(z)} \frac{F(r)}{\sqrt{1-F(r)^2}}\,\mathrm{d}r = z - z_0, \tag{54}$$

which solves $z$ as a function of the radius. The functions $F$ associated with the shapes **(i-iv)** are specified in Table (II). The geometrical differences between these profiles drawn for both $z$ and $\ell$ may be assessed in Fig. 4. Note that this figure exhibits the maximum and minimum radii.

`[Figure 4 about here]`

## IV. GENERALIZATION FOR SMALL WALL ADMITTANCES AND MOBILE WALLS

When the wall $\mathcal{W}_t$ is mobile or is not ideally rigid and lossless, the normal component of the acoustic velocity is no longer zero. Nevertheless, the wall $\mathcal{W}_t$ may still be described by $\mathcal{T}_{w,t}$ for a constant $u = w$, and the general notations Eq. (29) to Eqs. (31) remain valid. The only differencies are that $f|_w$ and $g|_w$ may be time-varying and that $\epsilon|_w \neq 0$ since the wall condition ($\widetilde{\mathbf{v}}.\mathbf{w_s}|_w \neq 0$) prevents isobars from being orthogonal to $\mathcal{W}_t$ In this case, the boundary conditions on $\mathcal{W}_t$ may be described by a relation linking $\widetilde{p}$ and $\widetilde{\mathbf{v}}.\mathbf{w_s}|_w$. Such a relation is usually specified in the Fourier domain using a *wall admittance* $Y$.

As an example, if a quasi-planar wall is vibrating, a standard boundary condition may be described for $= uw$ by[15] (page 47)

$$\partial_{\mathbf{w_s}}\widehat{p} + \frac{i\omega}{c} Y(\omega)\,\widehat{p} = -i\omega\rho_0\widehat{\mathbf{V}}.\mathbf{w_s}, \tag{55}$$

where $\partial_{\mathbf{w_s}} = \mathbf{w_s}.\mathbf{grad}$ is the derivative in the direction $\mathbf{w_s}$, $Q \mapsto \widehat{Q}$ gives the Fourier transform defined for the time-pulsation $\omega$, and $\mathbf{V}$ is the local velocity of $\mathcal{W}_t$. $Y = \rho_0 c \left[\mathbf{w_s}.(\widehat{\mathbf{v}} - \widehat{\mathbf{V}})\right]\Big|_w / \widehat{p}$ is the specific admittance of the material constituting the wall. Note that $Y$ is ordinarily given such that $\mathbf{w_s}$ is outwardly directed, so that a particular attention must be paid to the conventions used. Note that this direction is achieved choosing $g|_w \geq 0$ and $f|_w$ such that the inside of the guide is at the right side of $\mathbf{u_s}$.

This section establishes a mono-space wave equation in this general context for cases such that $\epsilon|_w \ll 1$, making $\epsilon^2|_w$ and $\epsilon^3|_w$ negligible. Note that this restriction encompasses yet many physical cases for which the wall admittance and so $\partial_{\mathbf{w_s}}\widetilde{p}|_w$ are small, as clarified below by Eq. (56). The reason for this restriction is also detailed.

### A. Derivation of the 1D-model

Establishing a 1D-model from Eq. (20) requires coping with two problems. The first one consists of making the boundary condition usable, exhibiting a relation between $\epsilon|_w$ and $\partial_{\mathbf{w_s}}\widetilde{p}$. This stage stands in for the simplification run in Sec. III considering that $\epsilon = 0$. Projecting Eq. (19) on $\mathbf{w_s}$ leads to this requisite identification given by

$$\epsilon = \sigma_s \frac{\partial_{\mathbf{w_s}}\widetilde{p}}{\partial_s \widetilde{p}}. \tag{56}$$

The persisting main problem is the evaluation of $\partial_u \phi/(\sigma_u \cos\delta)$ on $\mathcal{W}_t$. Once again, the local quasi-sphericity of isobars near the wall makes the solution of the propagation problem separate from that the geometry of isobars. Actually, this hypothesis is obtained as in Sec. III B. The only noteworthy differences are that a point $M(s,t)$ of $\mathcal{W}_t$ indexed by $s$ may be animated, and that $\epsilon|_w$ is not required to be zero. Nevertheless, all the definitions and the calculations (Eq. (32) to Eq. (41)) remain exact, adapting the notations as illustrated in Fig. 5, and considering $O_{s,t}$, $z_{O_{s,t}}$, $R_{s,t}$ in place of $O_s$, $z_{O_s}$, and $R_s$ in the previous formula.

```
[Figure 5 about here]
```

Then, recalling that $\delta = \phi - \theta$, Eq. (41) yields

$$\left.\frac{\partial_u \phi}{\sigma_u \cos\delta}\right|_w = \left.\frac{\cos\theta + \epsilon \sin\theta}{g}\right|_w. \tag{57}$$

Using Eq. (56) and neglecting $\epsilon^2$ and $\epsilon^3$ in $A_{s,s}$ and $A_s$, the hypothesis of quasi-sphericity Eq. (57) leads after calculations to

$$\begin{aligned} &B_{s,s}\partial_s^2\widetilde{p} + B_s\partial_s\widetilde{p} + B_{s,t}\partial_s\partial_t\widetilde{p} - \frac{1}{c^2}\partial_t^2\widetilde{p} \\ &+B_{\mathbf{w_s}}\partial_{\mathbf{w_s}}\widetilde{p} + B_{\mathbf{w_s},s}\partial_s\partial_{\mathbf{w_s}}\widetilde{p} + B_{\mathbf{w_s},t}\partial_t\partial_{\mathbf{w_s}}\widetilde{p} \;=\; 0, \end{aligned} \tag{58}$$

where

$$B_{s,s} = (1-\xi_s^2)/\sigma_s^2, \tag{59a}$$

$$B_s = \frac{2-\xi_n^2}{\sigma_s^2}\partial_s \ln g - \frac{1-\xi_n^2}{\sigma_s^2}\partial_s \ln \sigma_s - \frac{1}{2}\partial_s\left(\frac{\xi_s^2-\xi_n^2}{\sigma_s^2}\right) + \frac{1}{c}\partial_t\left(\frac{\xi_s}{\sigma_s}\right), \tag{59b}$$

$$B_{s,t} = 2\frac{\xi_s}{c\sigma_s}, \tag{59c}$$

$$B_{\mathbf{w_s}} = \frac{2-\xi_n^2}{g}\cos\theta + \frac{1-2\xi_n^2}{\sigma_s}\partial_s\theta - \frac{\xi_s}{\sigma_s}\partial_s\xi_n + \frac{1}{c}\partial_t\xi_n, \tag{59d}$$

$$B_{\mathbf{w_s},s} = -2\xi_s\xi_n/\sigma_s, \tag{59e}$$

$$B_{\mathbf{w_s},t} = 2\xi_n/c, \tag{59f}$$

are all evaluated for $u = w$. Finally, Eq. (58) and boundary conditions such as Eq. (55) furnish a 1D-model of the waveguide. As analysed in Sec. III D, the validity of this 1D-model is still limited to walls having a small curvature. This assumption holds only if $\partial_s\theta|_w$ is negligible. Practically, $B_{\mathbf{w_s}}$ may be well approximated by

$$B_{\mathbf{w_s}} = \frac{2-\xi_n^2}{g}\cos\theta - \frac{\xi_s}{\sigma_s}\partial_s\xi_n + \frac{1}{c}\partial_t\xi_n. \tag{60}$$

Particular derivations for visco-thermal losses on the wall or for mobile walls are described below. Beforehand, the requirement $\epsilon|_w \ll 1$ is clarified.

## B. Geometrical hypothesis and compatibility with the problem

Let $\mathcal{P}$ describe the problem associated with the propagation in a given waveguide for which the wall conditions are linear with respect to the pressure. The linearity of the wave equation Eq. (3) and of the wall conditions ensures that of the acoustic propagation in the guide. Consequently, for such conditions, the exactness of the establishment of Eq. (20) and Eq. (56) guarantees the preservation of this property. However, if $\widetilde{p}_1$ and $\widetilde{p}_2$ are two solutions of these equations, $\widetilde{p} = \widetilde{p}_1 + \lambda\widetilde{p}_2$ does not appear as an evident solution. Only $\lambda\widetilde{p}_1$ or $\lambda\widetilde{p}_2$ appears evident when the motion of $\mathcal{W}_t$ is imposed. These peculiar properties are now described and investigated.

Under the linearity assumption of the wall conditions, the operator $\widetilde{p} \mapsto \lambda\widetilde{p}$ keeps $\epsilon$ invariant (see Eq. (56)). Then, it acts on the first member of Eq. (20) as a multiplication by $\lambda$ (first order homogeneity) for imposed $\xi_s$ and $\xi_n$. This proves that, for any solution $\widetilde{p}$ of a problem $\mathcal{P}$, $\lambda\widetilde{p}$ is also a solution. On the contrary, making the operator $(\widetilde{p}_1, \widetilde{p}_2) \mapsto \widetilde{p}_1 + \lambda\widetilde{p}_2$ act on Eq. (20) and Eq. (56) does not lead to such remarkable relations. This is not a paradox but is simply due to the writing of $\mathcal{P}$ in the isobaric coordinate system. This indicates that the inherent linearity of $\mathcal{P}$ involves explicitly the coupling between the propagation and the geometry of isobars: multiplying a solution pressure by $\lambda$ does not change the isobaric map, but another change of solution does. More precisely, it gives information about $\partial_u\phi/\sigma_u$ for which the compatibility with the quasi-sphericity hypothesis requires study.

Starting from Eq. (20) and Eq. (56), the exact wave equation for the problem $\mathcal{P}$ may be written as the nullity of the sum of three terms $T_{ne}[\widetilde{p}]$, $T_{nl}[\widetilde{p}]$, and $T_l[\widetilde{p}]$ defined below. $T_{ne}[\widetilde{p}]$ corresponds to the term of Eq. (20) which is non evaluable for $u = w$ from the single geometry of the wall. It corresponds to

$$T_{ne}[\widetilde{p}] = (1 - \xi_n^2)\left[1 + \left(\frac{\sigma_s \partial_{\mathbf{w_s}}\widetilde{p}}{\partial_s\widetilde{p}}\right)^2\right] \frac{\partial_u\phi}{\sigma_u \cos\delta}\frac{\partial_s\widetilde{p}}{\sigma_s}, \tag{61}$$

for which it is recalled that $\partial_u\phi/\sigma_u$ is the only quantity non evaluable on $\mathcal{W}_t$, and where $\cos\delta$ is not developed using $\partial_{\mathbf{w_s}}\widetilde{p}$ and $\partial_{\mathbf{u_s}}\widetilde{p}$ to keep the formula compact. $T_{nl}[\widetilde{p}]$ contains all other terms which are non linear in $\epsilon$, and is given by

$$\begin{aligned} T_{nl}[\widetilde{p}] &= (1 - \xi_n^2)\left[\left(\frac{\partial_{\mathbf{w_s}}\widetilde{p}}{\partial_s\widetilde{p}}\right)^2 \big(\sigma_s\partial_s\theta\,\partial_{\mathbf{w_s}}\widetilde{p} + \partial_s\mathrm{ln}\sigma_s\,\partial_s\widetilde{p}\right. \\ &\qquad \left. -\partial_s^2\widetilde{p}\big) + 2\frac{\partial_{\mathbf{w_s}}\widetilde{p}}{\partial_s\widetilde{p}}\partial_s\partial_{\mathbf{w_s}}\widetilde{p}\right]. \end{aligned} \tag{62}$$

The remaining term $T_l[\widetilde{p}]$ is only constituted of linear terms evaluable for $u = w$: all the first order terms such as $-2\,\xi_n\xi_s\,\epsilon\,\partial_s^2\widetilde{p}\,/\,\sigma_s^2$ in $A_{s,s}$, or $2\,\xi_n\,\epsilon\,\partial_s\partial_t\widetilde{p}\,/\,(c\sigma_s)$ in $A_{s,t}$, vanish with those of $A_s$ when signifying $\epsilon$. $T_l[\widetilde{p}]$ would exactly correspond to the first member of Eq. (58) omitting the contribution in $B_s$ and $B_{\mathbf{w_s}}$ of $T_{ne}$ after using the quasi-sphericity hypothesis.

Defining $T[\widetilde{p}] = T_{ne}[\widetilde{p}] + T_{nl}[\widetilde{p}] + T_l[\widetilde{p}]$, the wave equation is obtained writing $T[\widetilde{p}] = 0$. The condition of linearity is then obtained writing

$$T[\widetilde{p}_1 + \lambda\widetilde{p}_2] = T[\widetilde{p}_1] + \lambda T[\widetilde{p}_2], \tag{63}$$

for all $\widetilde{p}_1$ and $\widetilde{p}_2$ solutions, and for all $\lambda$. When $\xi_s$ and $\xi_n$ are unchanged for distinct solutions (for instance, rigid but controlled mobile walls), $T_l$ is linear so that this condition is reduced to Eq. (63) taking $T[\widetilde{p}] = (T_{ne}[\widetilde{p}] + T_{nl}[\widetilde{p}])/(1-\xi_n^2)$. Equation (63) exhibits the non linear relation between the three geometrical coefficients $(\partial_u\phi/\sigma_u)_{\mathcal{P}}$ associated with the problem $\mathcal{P}$ for the pressures $\widetilde{p} = \widetilde{p}_1$, $\widetilde{p}_2$, $\widetilde{p}_1 + \lambda\widetilde{p}_2$, and these three pressures.

The quasi-sphericity hypothesis does not mostly satisfy this condition since it makes $(\partial_u\phi/\sigma_u)|_w$ depend only on the wall geometry but not on the pressure. As a consequence, the linearity of the 1D-modelling for this hypothesis requires $\epsilon|_w \ll 1$ so that the induced nonlinear terms may be neglected, leading to Eq. (58).

### C. Influence of mobile walls

Equation (58) can be straightforwardly used to establish a 1D-modelling for a controlled mobile wall.

From Eq. (10a) and Eq. (11a), the time derivatives of $\mathbf{u_s}$ and $\mathbf{w_s}$ are obtained for

$$\partial_t \mathbf{u_s} = \partial_t\theta\,\mathbf{w_s}, \tag{64a}$$

$$\partial_t \mathbf{w_s} = -\partial_t\theta\,\mathbf{u_s}. \tag{64b}$$

Since from Eqs. (14) $\mathbf{V}/c = \xi_s\,\mathbf{u_s} + \xi_n\,\mathbf{w_s}$, the acceleration $\partial_t\mathbf{V}$ is such that

$$\partial_t\left(\frac{\mathbf{V}}{c}\right) = (\partial_t\xi_s - \xi_n\partial_t\theta)\mathbf{u_s} + (\partial_t\xi_n + \xi_s\partial_t\theta)\mathbf{w_s}. \tag{65}$$

As $\partial_{\mathbf{w_s}}\widetilde{p} = \mathbf{w_s}.\mathbf{grad}(\widetilde{p})$, Eq. (2) and Eq. (65) yields

$$\partial_{\mathbf{w_s}}\widetilde{p} = -\rho_0 c(\partial_t\xi_n + \xi_s\partial_t\theta). \tag{66}$$

Equation (66), evaluated on the wall, and Eq. (58) furnish the 1D-model.

When $\xi_s \ll 1$ and $\xi_n \ll 1$, the quantities $1-\xi_s^2$ and $2-\xi_n^2$ appearing in $B_{s,s}$, $B_s$, and $B_{\mathbf{w_s}}$ may be approximated by 1 and 2. Describing $\mathcal{W}_t$ with $\mathcal{R}(\ell,t) = g|_w(\ell,t)$, $\ell$ being the curvilinear ordinate such that $\sigma_s|_w(\ell,t) = 1$, the model takes the simpler form

$$\begin{aligned}
&\partial_\ell^2\widetilde{p} + \left(2\frac{\partial_\ell\mathcal{R}}{\mathcal{R}} + \frac{\partial_t\xi_s}{c} + \partial_\ell(\xi_n^2 - \xi_s^2)\right)\partial_\ell\widetilde{p} + 2\frac{\xi_s}{c}\partial_t\partial_\ell\widetilde{p} - \frac{1}{c^2}\partial_t^2\widetilde{p} \\
&= \rho_0 c\left[\left(\frac{2\cos\theta}{\mathcal{R}} + \frac{\partial_t\xi_n}{c} - \xi_s\partial_\ell\xi_n\right) - 2\xi_s\xi_n\partial_\ell + 2\frac{\xi_n}{c}\partial_t\right] \\
&\quad(\partial_t\xi_n + \xi_s\partial_t\theta),
\end{aligned} \tag{67}$$

where the geometrical quantities are still evaluated for $u = w$ and the second member may be interpreted as sources induced by the motion of $\mathcal{W}_t$.

Note that for many practical cases, the controlled motion or the vibrations of the wall are sufficiently small to consider much stronger approximations. Under such adapted conditions, Eq. (67) may be reduced to its first order approximation

$$\partial_\ell^2 \widetilde{p} + 2\frac{\partial_\ell \mathcal{R}}{\mathcal{R}}\partial_\ell \widetilde{p} - \frac{1}{c^2}\partial_t^2 \widetilde{p} = \rho_0 c \frac{2\cos\theta}{\mathcal{R}}(\partial_t \xi_n + \xi_s \partial_t \theta), \tag{68}$$

for $u = w$. For vibrating walls, this last acoustic equation may be coupled with the model of the wall vibrations.

### D. Influence of visco-thermal losses

Equation (58) also enables treating the case of large pipes with visco-thermal losses due to the wall, now assumed motionless.

Let significant parameters specifying the properties and the nature of the fluid at rest be defined: the coefficient of shear viscosity $\mu$, the coefficient of thermal conductivity $\lambda$, the heat coefficients at constant pressure and constant volume per unit of mass $C_P$ and $C_V$, the specific heat ratio $\gamma = C_P/C_V$, and finally the characteristic lengths $l'_v = \mu/(\rho_0 c)$ and $l_h = \lambda/(\rho_0 c C_P)$. The effect of the visco-thermal losses on the acoustics may be described for travelling waves by an equivalent specific wall admittance $Y$ given by[15] (pages 112-115)

$$Y(\omega, s) = \left(\frac{i\omega}{c}\right)^{\frac{1}{2}} \left[\kappa(s)\sqrt{l'_v} + (\gamma - 1)\sqrt{l_h}\right], \tag{69}$$

where $\kappa$ is linked to the angle of incidence of the wavefronts on $\mathcal{W}_t$ as described below. Note that to be physically meaningful, $Y$ may have an hermitian symmetry so that the complex $(i\omega)^{1/2}$ needs to be specified: this quantity may be understood as $\sqrt{|\omega|}\,\exp(i\pi/4)$ for $\omega \geq 0$, and the conjugate $\sqrt{|\omega|}\,\exp(-i\pi/4)$ for $\omega < 0$. More precisely, this definition makes it correspond to the time operator $\partial_t^{1/2}$ for causal functions[16].

The validity of Eq. (69) relies on the fact that the thickness of the boundary layer may be very small with regard to both the radius and the radius of curvature of $\mathcal{W}$. For a pulsation $\omega$, the thickness is given by $\sqrt{2c\, l'_v/\omega}$ for the viscous effects, and $\sqrt{2c\, l_h/\omega}$ for the thermal effects. For usual conditions, $l'_v$ and $l_h$ are about $4\ 10^{-8}$m and $6\ 10^{-8}$m so that the thermal effects are the most restrictive. The thickness decreases with the frequency $f$ as $f^{-1/2}$ and is about 2.5 mm at $f = 1$ Hz for the thermal effects. This condition is then fulfilled for many practical cases.

Now, $\kappa(s)$ corresponds to the square of the sine of the angle[15] (page 155) $(\mathbf{u_s}, \mathbf{grad}(\widetilde{p}))$, or identically, to $\cos^2\delta = 1/(1-\epsilon^2)$. As $\epsilon^2$ is neglected above, $\kappa$ may be approximated by 1. Then, if $\mathbf{w_s}$ is outwardly directed, the boundary condition Eq. (55) (for $\mathbf{V}=\mathbf{0}$) may be written in the time domain by

$$\partial_{\mathbf{w_s}}\widetilde{p} + \frac{\sqrt{l'_v} + (\gamma-1)\sqrt{l_h}}{c^{\frac{3}{2}}}\partial_t^{3/2}\widetilde{p} = 0, \tag{70}$$

where for usual conditions $\sqrt{l'_v} + (\gamma-1)\sqrt{l_h}$ is about $3\ 10^{-4}\mathrm{m}^{\frac{1}{2}}$. This order of magnitude confirms that the effect due to the boundary layer is small so that the assumption $\epsilon \ll 1$ is well founded in this case, and the quasi-sphericity hypothesis compatible with the problem.

Finally, the dominating requirement is the slowness of the variation of the cross-section of the pipe. The 1D-model obtained for these pipes from Eq. (58) and Eq. (70) with $\xi_s|_w = \xi_n|_w = 0$ is given for $u = w$ by

$$\frac{1}{\sigma_s^2}\partial_s^2\widetilde{p} + \frac{2\,\partial_s \ln g}{\sigma_s^2}\partial_s\widetilde{p} - \frac{1}{c^2}\partial_t^2\widetilde{p} - \frac{2\,\cos\theta}{g}\,\frac{\Gamma}{c^{\frac{3}{2}}}\,\partial_t^{\frac{3}{2}}\widetilde{p} = 0, \tag{71}$$

where $\Gamma = \sqrt{l'_v} + (\gamma-1)\sqrt{l_h}$. For the ordinate $\ell$ for which $\sigma_s|_w = 1$, this equation appears as a Webster equation perturbed by the low fractional differential term $2\frac{\cos\theta}{c^{\frac{3}{2}}g}\Gamma\,\partial_t^{\frac{3}{2}}\widetilde{p}$. Note that for the profile $g|_w(s) = R_0$, this equation exactly yields the well-known equation of plane waves guided in large cylindric tubes with visco-thermal losses[15] (page 145).

## V. CONCLUSION

A rigorous derivation of the linear acoustic wave equation in any local isobaric coordinate system has been presented for axisymmetric problems. As the main theoretical result of this work, it exhibits formally the exact coupling between the geometry of the wavefronts and the propagation of the pressure. Straightforward derivations have shown that any regular isobaric map may satisfy a purely geometrical criterion of admissibility. The general time-invariant isobaric maps have been proven to be parallel planes, coaxial cylinders, and concentric spheres. Other immobile invariant maps exist but, in this case, only a pure sinusoid or a pure exponential can travel on each of them. Furthermore, the isobaric wave equation shows that separating the resolution of the isobaric map from that of the 1D-pressure is usually impossible. Assuming the quasi-sphericity near the wall for a minimal order is proven to be sufficient to dispose of this problem. The 1D-models derived for motionless rigid walls or mobile ones with small admittances constitute the second main results of this work. They make the arc length of the wall appear as the natural distance travelled by a wave with the speed $c$.

Even if the geometrical hypothesis does not require fixed wavefronts as usual, the limitations mostly remain those of the classical Webster equation, namely, low curved and smooth walls, and sufficiently large wavelengths ensuring that transverse modes are not excited. To quantify the quality of the 1D-models, a numerical validation must be run, comparing the pressure deduced for them to that computed near the wall thanks to finite element methods or using the discrete model of Pagneux[10]. In particular, the horns presented in Sec. III E could be tested for an excitation $\widetilde{p}(0,t)$ at the input $s=0$ and for a given load admittance at the output $s=L$ such as that of divergent spherical waves. For the 2D-algorithms, the same boundary conditions may be taken on the spheres orthogonal to the wall in $s=0$ and $s=L$, the quasi-sphericity hypothesis being appropriate to this geometry. Other meaningful comparisons with 2D-models may be done for boundary conditions which are compatible with the quasi-sphericity hypothesis and adaptable to 1D-models (e.g. radiating portion of a sphere[15] (page 246)).

Nevertheless, whatever the success of a numerical validation, this work can expanded to other models having a mono-spatial dependence, which would exceed the above-mentioned limitations. Indeed, starting from the general rigorous equation Eq. (20), geometrical hypotheses more relaxed than that of the quasi-sphericity could be used. Mainly, choosing hypotheses of higher orders is an interesting prospect. A particularly interesting one is an order of regularity and of flexibility imposed on the wavefront geometry by $\partial_{\mathbf{u_u}}^K \phi\big|_w = 0$ (with $\partial_{\mathbf{u_u}} = \frac{1}{\sigma_u}\partial_u$) for a given $K \geq 2$ ($K=0$ would impose the wrong angle $\phi|_w = 0$, and $K=1$ would impose quasi-planar wavefronts near the wall rather than the more appropriate quasi-spherical ones). But such alternatives involve an extensive investigation. Indeed, establishing the associated 1D-models requires solving the system of equations obtained by applying $X \mapsto \partial_{\mathbf{u_u}}^k X\big|_w$ on Eq. (20) for $k = 0, 1, ..., K-1$, the hypothesis being used in the last equation. A careful study of fundamental properties such as the linearity or the compatibility with the symmetry of the problem must be performed since they are not guaranteed a priori. In addition to the relaxation of the above mentioned constraints induced by the quasi-sphericity hypothesis, the main interest of this extension is potentially having control of the input-output isobar geometry through the $K-1$ integrating constants linked to the $\partial^k_{\mathbf{u_u}}\phi\big|_w$. In this case, the corresponding 1D-models account for the propagation of the pressure as well as that of the geometrical information represented.

## Acknowledgements

The research reported here is based uppon a doctoral dissertation completed by the author at the University of Paris XI. I wish to thank my advisor X. Rodet, the Analysis-Synthesis team of IRCAM, and the ministry of research for supporting this research. I am very grateful to J. Kergomard and C. Vergez for their critical reading of this manuscript, as well as M. Lo Cascio for proofreading.

## References

[1] D. Bernoulli, Sur le son et sur les tons des tuyaux d'orgues différemment construits (Physical, Mechanical and Analytical Researches on Sound and on the Tones of Differently Constructed Organ Pipes), Mém. Acad. Sci. (Paris), 1764, (in French, reference extracted from the paper of Eisner[4]).

[2] J. L. Lagrange, Nouvelles recherches sur la nature et la propagation du son (New Researches on the Nature and Propagation of Sound), Misc. Taurinensia (Mélanges Phil. Math., Soc. Roy. Turin), 1760-1761, (in French, reference extracted from the paper of Eisner[4]).

[3] A. G. Webster, "Acoustical impedance, and the theory of horns and of the phonograph," Proc. Nat. Acad. Sci. U.S. **5**, 275–282 (1919), errata, ibid. **6**, p.320 (1920).

[4] E. Eisner, "Complete solutions of the "Webster" horn equation," J. Acoust. Soc. Amer. **41**(4), 1126–1146 (1967).

[5] R. F. Lambert, "Acoustical studies of the tractrix horn. I," J. Acoust. Soc. Amer. **26**, 1024–1028 (1954).

[6] E. S. Weibel, "On Webster's horn equation," J. Acoust. Soc. Amer. **27**, 726–727 (1955).

[7] A. H. Benade and E. V. Jansson, "On plane and spherical waves in horns with nonuniform flare. I. Theory of radiation, resonance frequencies, and mode conversion," Acustica **31**, 79–98 (1974).

[8] G. R. Putland, "Every one-parameter acoustic field obeys Webster's horn equation," J. Audio Eng. Soc. **6**, 435–451 (1993).

[9] A. F. Stevenson, "Exact and approximate equations for wave propagation in acoustic horns," J. Appl. Phys. **22**(12), 1461–1463 (1951).

[10] V. Pagneux, N. Amir, and J. Kergomard, "A study of wave propagation in varying coss-section waveguides by modal decomposition. part I. Theory and validation.," J. Acoust. Soc. Am. **100**(4), 2034–2048 (1996).

[11] J. Agulló, A. Barjau, and D. H. Keefe, "Acoustic propagation in flaring, axisymmetric horns: I. A new family of unidimensional solutions," Acustica **85**, 278–284 (1999).

[12] P. M. Morse and K. U. Ingard, *Theoretical acoustics* (McGraw-Hill, New York, 1968).

[13] D. P. Berners, "Acoustics and signal processing techniques for physical modeling of brass instruments," Ph.D. thesis, Standford University, 1999.

[14] *Handbook of mathematical functions*, edited by M. Abramowitz and I. A. Stegun (Dover publications, inc., New York, 1970).

[15] M. Bruneau, *Manuel d'acoustique fondamentale, études en mécanique des matériaux et des structures* (Hermès, Éditions HERMÈS, 8 quai du Marché-Neuf, 75004 Paris, FRANCE, 1998).

[16] D. Matignon, "Stability properties for generalized fractional differential systems," ESAIM Proceedings **5**, 145–158 (1998), `http://www.edpsciences.org/articles/proc/Vol.5/index.htm`.

Table I: List of symbols

| | |
|---|---|
| $\rho_0$ | density of air |
| $c$ | speed of sound in air |
| $\begin{cases} z = f(s,u,t) \\ r = g(s,u,t) \end{cases}$ | time-varying change of spatial coordinates |
| $p(z,r,t)$, $\widetilde{p}(s,u,t)$ | acoustic pressure located at $(z,r,t)$ and $(s,u,t)$ respectively |
| $\mathbf{v}(z,r,t)$ | particle acoustic velocity located at $(z,r,t)$ |
| $\mathcal{I}_{s,t}$ | isobars indexed by $s$ at the time $t$ |
| $\mathcal{T}_{u,t}$ | axisymmetric surfaces indexed by $u$ at the time $t$ |
| $\mathcal{W}_t$ | wall of the guide at the time $t$ |
| $\mathbf{u_z}$, $\mathbf{u_r}$ | unitary vectors associated with the longitudinal $(z)$ and the transverse $(r)$ coordinates of the cylindric basis |
| $\mathbf{u_s}(s,u,t)$, $\mathbf{u_u}(s,u,t)$ | field of unitary vectors tangent to $\mathcal{I}_{s,t}$ and $\mathcal{T}_{u,t}$ respectively |
| $\mathbf{w_s}(s,u,t)$, $\mathbf{w_u}(s,u,t)$ | vectors $\mathbf{u_s}(s,u,t)$ and $\mathbf{u_u}(s,u,t)$ rotated from $+\pi/2$ |
| $\sigma_s(s,u,t)$, $\sigma_u(s,u,t)$ | norms of the vectors of the basis induced by the change $(f,g)$ for the coordinates $s$ and $u$ respectively |
| $\xi_s(s,u,t)$, $\xi_n(s,u,t)$ | Mach numbers of a point located at $(s,u)$ for the orthogonal directions $\mathbf{u_s}$ and $\mathbf{w_s}$ |
| $\theta(s,u,t)$, $\phi(s,u,t)$, and $\delta(s,u,t)$ | oriented angles $(\mathbf{u_z},\mathbf{u_s})$, $(\mathbf{u_r},\mathbf{u_u})$, and $(\mathbf{w_s},\mathbf{u_u})$ respectively |
| $\partial_z^k$ | partial derivative with respect to $z$ of order $k$ |
| **grad** | gradient operator |
| div | divergence operator |
| $\partial_{\mathbf{w_s}} = \mathbf{w_s}.\mathbf{grad}$ | partial derivative in the direction $\mathbf{w_s}$ |
| $\Delta$ | Laplacian operator |

| case | $F(R)$ | $R^*$ |
|---|---|---|
| (i) $\alpha > 0$ | $\alpha R$ | $\alpha^{-1}$ |
| (ii) $\alpha > 0$ | $\alpha\sqrt{R^2 - {R_0}^2}$ | $\sqrt{{R_0}^2 + \alpha^{-2}}$ |
| (iii) $\alpha > 0$ | $\alpha\sqrt{{R_0}^2 - R^2}$ | $\sqrt{{R_0}^2 - \alpha^{-2}}$ if $\|\alpha R_0\| \geq 1$ |
| (iv) $\alpha \neq 0$ $\alpha \neq 1$ | $\alpha {R_0}^{\frac{1}{\alpha}} R^{\frac{\alpha-1}{\alpha}}$ | $R_0^{\frac{1}{1-\alpha}} \|\alpha\|^{\frac{\alpha}{1-\alpha}}$ |

Table II: This table sums up for the cases **(i-iv)** the expression of $F$ used to compute $\mathcal{R}'$ from $\mathcal{R}$, and the minimum (**iii,iv** $0 < \alpha < 1$)) or maximum (**i,ii,iv** $\alpha \notin [0, 1]$) radius $R^*$ for which an infinite slope is reached on the physical shape.

## List of Figures

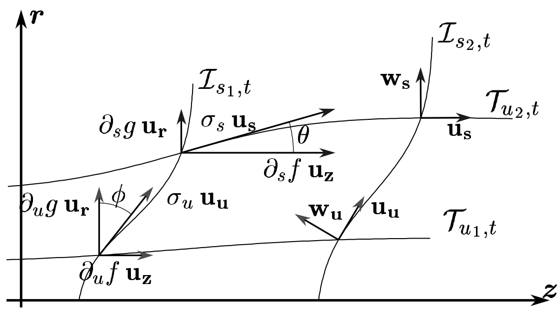


Figure 1: Definition of the geometrical quantities related to the local basis $\mathcal{B}_t$. Note that although all represented vectors and angles coexist in every point located at $(s, u)$, various quantities are described in several distinct points to improve the clarity and the legibility of the figure.

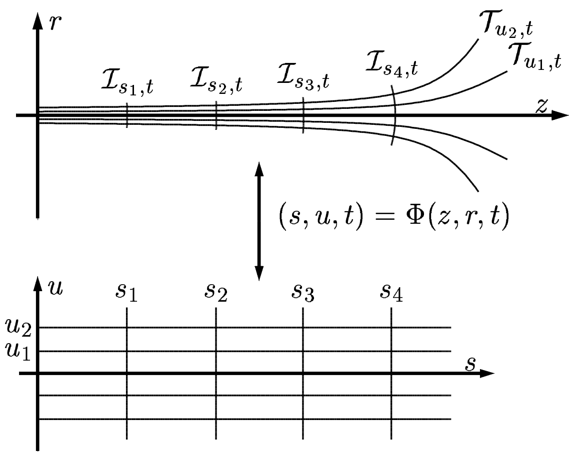


Figure 2: This figure gives an example of a change of coordinates which rectifies the isobaric maps at a given time $t$, and for which $u$ indexes the field lines. For the coordinate system $(s, u)$, the pressure does not vary with $u$. In this illustration, the simple topology of isobars $(\mathcal{I}_{s,t})$ makes the definition of the diffeomorphism $\Phi$ possible over all the map. When more complex topologies appear (closed curves, singular points, splitting curve, etc...), several changes of coordinates should be considered on local domains. The study of a global resolution for such topologies is not discussed here.

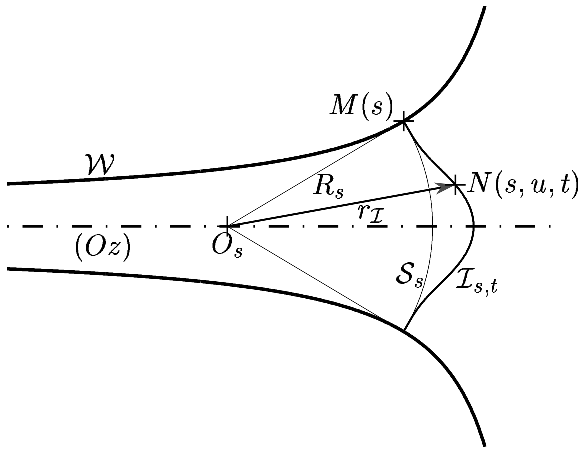


Figure 3: $O_s(s) \in (Oz)$ and $R_s(s)$ are the center and the radius of the sphere $\mathcal{S}_s$ tangent to $\mathcal{I}_{s,t}$ in $M(s) \in \mathcal{W}$. $r_{\mathcal{I}}(s,u,t)$ is the distance between $O_s$ and the point $N \in \mathcal{I}_{s,t}$ located at $(s,u,t)$. It is assumed that $\mathcal{I}_{s,t}$ and $\mathcal{S}_s$ are close at the second order in $M(s)$. Namely, for each $(s,t)$, $u \mapsto r_{\mathcal{I}}(s,u,t)$ may be approximated by the constant $R(s)$ at the second order for $u$ in the vicinity of $w$.

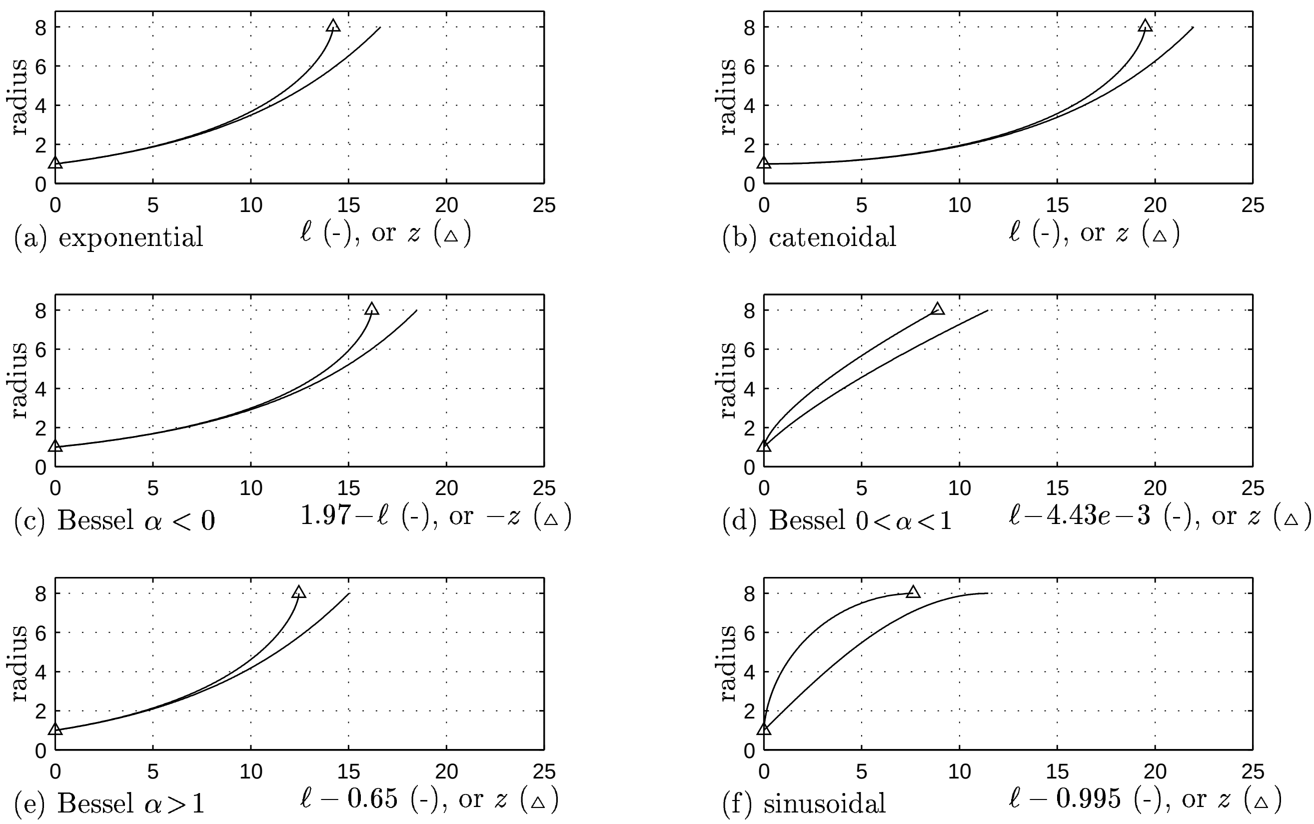


Figure 4: The profiles corresponding to the cases **(i-iv)** are drawn for both the $\ell$-ordinate (-), and the $z$-ordinate ($\triangle$). Parameters are computed so that $R^*$ is reached, $R_{min} = 1$ unit, and $R_{max} = 8$ units: (a) $R_0 = 1$, $\alpha = 1/8$, (b) $R_0 = 1$, $\alpha = 1/\sqrt{63}$, (c) $R_0 \approx 8.6e-3$, $\alpha = -10$, (d) $R_0 \approx 0.381$, $\alpha \approx 0.743$ (computed to have the same length for (d) and (f)), (e) $R_0 \approx 0.745$, $\alpha = 10$, (f) $R_0 = 8$, $\alpha = 1/\sqrt{63}$. Appropriate translations in $\ell$ (and a symmetry for (d)) are used to make the profiles increasing and starting at $\ell = z = 0$.

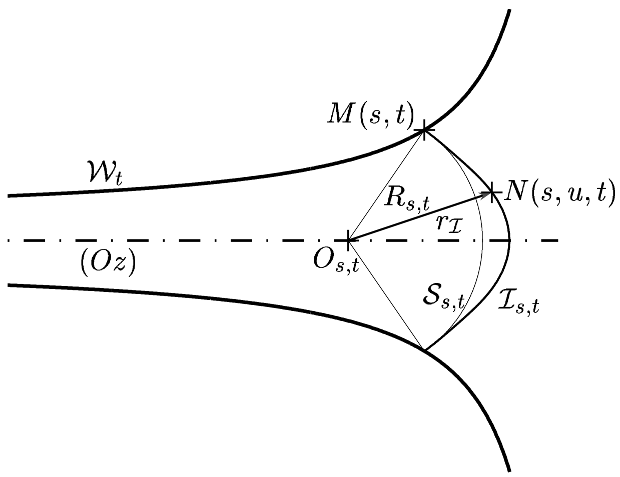


Figure 5: When the wall is not rigid, motionless, and lossless, isobars are not necessarily orthogonal to the wall. The hypothesis of their quasi-sphericity near the wall may be yet considered in this more general case. Note that the spheres $\mathcal{S}_{s,t}$ tangent to isobars $\mathcal{I}_{s,t}$ now move with respect to the angle $\phi(s,w,t)$ which is no longer a right angle. Nevertheless, the formula of definition Eq. (32) to Eq. (41) are not modified: the only differences are that $O_s$, $z_{O_s}$, and $R_s$ may now depend on the time.